ARTICLE
Journal of Cellular Biochemistry 112:3762–3772 (2011)

Journal of Cellular Biochemistry

Use of Monocyte/Endothelial Cell Co-Cultures (In Vitro) and a Subcutaneous Implant Mouse Model (In Vivo) to Evaluate a Degradable Polar Hydrophobic Ionic Polyurethane

Sarah M. McDonald,[1,2] Loren A. Matheson,[2,3] Joanne E. McBane,[4] Drew Kuraitis,[1,2] Erik Suuronen,[1,2] Joseph Paul Santerre,[4] and Rosalind S. Labow[1,2*]

[1] *University of Ottawa, Ottawa, Ontario, Canada*
[2] *Division of Cardiac Surgery, University of Ottawa Heart Institute, Ottawa, Ontario, Canada*
[3] *Department of Pediatrics, University of Saskatchewan, Saskatoon, Saskatchewan, Canada*
[4] *Institute of Biomaterials and Biomedical Engineering, University of Toronto, Toronto, Ontario, Canada*

ABSTRACT

Potential benefits of co-culturing monocytes (MC) with vascular smooth muscle cells have been reported on for tissue engineering applications with a degradable, polar, hydrophobic, and ionic polyurethane (D-PHI). Since the interaction of MC and endothelial cells (EC) within the blood vessel endothelium is also a process of wound repair it was of interest to investigate their function when cultured on the synthetic D-PHI materials, prior to considering the materials' use in vascular engineering. The co-culture (MC/EC) in vitro studies were carried out on films in 96 well plates and porous scaffold disks were prepared for implant studies in an in vivo subcutaneous mouse model. After 7 days in culture, the MC/EC condition was equal to EC growth but had lower esterase activity (a measure of degradative potential), no pro-inflammatory TNF-α and a relatively high anti-inflammatory IL-10 release while the ECs maintained their functional marker CD31. After explantation of the porous scaffolds, a live/dead stain showed that the cells infiltrating the scaffolds were viable and histological stains (May-Grunwald, Trichrome) demonstrated tissue in growth and extracellular matrix synthesis. Lysates from the implant scaffolds analyzed with a cytokine antibody array showed decreased pro-inflammatory cytokines (IL-6, TNF-α, GM-CSF), increased anti-inflammatory cytokines (IL-10, IL-13, TNF-RI), and increased chemotactic cytokines (MCP-1, MCP-5, RANTES). The low foreign body response elicited by D-PHI when implanted in vivo supported the in vitro studies (EC and MC co-culture), demonstrating that D-PHI promoted EC growth along with an anti-inflammatory MC, further demonstrating its potential as a tissue engineering scaffold for vascular applications. J. Cell. Biochem. 112: 3762–3772, 2011.

KEY WORDS: ENDOTHELIAL CELL; MONOCYTE/MACROPHAGE; CO-CULTURE; VASCULAR GRAFT; POLYURETHANE; SCAFFOLD IMPLANT

Tissue engineering remains a promising strategy through which the generation of a synthetic small diameter vascular graft may be produced. Various materials and regenerative techniques have been explored, yet to date, a commercially successful construct has not fully addressed this challenge (Kakisis et al., 2005). The need for such a graft is prevalent as peripheral vascular disease affects millions of people worldwide (Selvin and Erlinger, 2004). Current options for treatment are limited to surgical reconstruction of the diseased vessel, the use of stents, and in the worst cases, amputation (Goodney et al., 2009). The availability of a peripheral vascular graft scaffold for the purposes of tissue engineering a blood vessel would provide another much needed treatment option. In order for such a graft to be successful it must possess suitable mechanical properties while allowing for the regulated proliferation of vascular smooth muscle cells (VSMC) and endothelial cells (EC) which will ultimately comprise the new vessel (Stegemann and Nerem, 2003). In addition, the material should degrade at a controlled rate and most important elicit a low foreign

Grant sponsor: Canadian Institutes of Health Research Collaborative Health Program; Grant number: 337246-2007/CPG83459; Grant sponsor: Ontario Graduate Scholarship; Grant sponsor: Canadian Arthritis Network post-doctoral fellowship; Grant sponsor: Heart and Stroke Foundation Fellowship; Grant sponsor: Heart and Stroke Foundation Ontario Master's Studentship Award.

*Correspondence to: Dr. Rosalind S. Labow, PhD, University of Ottawa Heart Institute, 40 Ruskin Street, H5229, Ottawa, ON K1Y 4W7. E-mail: rlabow@ottawaheart.ca

Received 10 June 2011; Accepted 2 August 2011 • DOI 10.1002/jcb.23307 • © 2011 Wiley Periodicals, Inc.
Published online 8 August 2011 in Wiley Online Library (wileyonlinelibrary.com).

body reaction. The final scaffold should provide a three-dimensional structure on which isolated cells can adhere and proliferate to eventually form a functional blood vessel (Bonfield et al., 1989).

Understanding the interaction of the essential cells in the regeneration process both with each other and with the material scaffold is paramount. One such cell is the monocyte (MC). Whenever an artificial material is implanted in vivo, MC are recruited to the site (Anderson et al., 2008). The MC and MC-derived macrophages (MDM) then initiate either a wound healing or a pro-inflammatory foreign body response which can be influenced by the chemistry of the material (Anderson et al., 2008). Since the chemical structure of the material surface has been shown to influence the eventual phenotype of the MDM, the components of the graft material are of integral importance in determining the success of the graft itself. It is hypothesized that MDM which have adopted a wound healing phenotype will aid in cell recruitment and function in the process of tissue regeneration by secretion of the appropriate cytokines into their environment.

Monocyte chemotactic protein-1 (MCP-1) has been found to be important for the recruitment of the essential vascular cells (EC and VSMC) to a vascular graft in vivo (Roh et al., 2010). Both VSMC and EC proliferation and phenotype have been shown to be influenced by MC (Schubert et al., 2008). It is necessary that the proliferative phenotype of VSMC shift to the contractile phenotype when vessel regeneration occurs and that proper endothelialization of a graft lumen take place in order to ensure its overall patency (Konig et al., 2009). An appropriate EC layer is required in order to create an intraluminal surface similar to that of a native vessel which proactively protects against the risk of a thrombogenic event (Zilla et al., 2007).

A scaffold made of a degradable, polar, hydrophobic, and ionic polyurethane (D-PHI) has been conceived with specific attention given to its physical and chemical properties for peripheral vascular graft generation. The scaffold possesses high porosity (~75–80%) and pore interconnectivity for cell proliferation and previous studies have indicated that the scaffold was biocompatible and non-toxic to cells while possessing appropriate mechanical properties (Sharifpoor et al., 2009; Sharifpoor et al., 2010). In addition, D-PHI degraded in vivo and in vitro at a controlled rate which would allow for the time necessary for vessel regeneration (McBane et al., 2011a). It has been shown that cells adhere preferentially to hydrophilic surfaces; however, excessive hydrophilicity tends to decrease EC proliferation and adhesion (Zhu et al., 2002). D-PHI was formulated with monomers to produce a final product with balanced hydrophilic and hydrophobic character, with an end goal of optimizing cell adhesion and tissue regeneration within the porous structure.

D-PHI has demonstrated favorable characteristics in in vitro studies with two of the essential cells in vessel regeneration. When MC were cultured on D-PHI, the material promoted differentiation to a MDM wound healing phenotype where significantly more interleukin (IL)-10 was released over time than IL-1β and tumor necrosis factor (TNF)-α when compared with cells cultured on tissue culture polystyrene (McBane et al., 2009a). In addition, when MC were cultured with VSMC, the co-culture demonstrated increased cell attachment as assessed by DNA with the VSMC maintaining their contractile phenotype marker, calponin. Moreover, as with MC alone, there was an increased release of the anti-inflammatory cytokine IL-10 in the co-culture which resulted in a high IL-10/TNF-α ratio (McBane et al., 2011b).

Based on the encouraging results of D-PHI with MC alone (McBane et al., 2009a) and in co-culture with VSMC (McBane et al., 2011b), D-PHI was assessed in this study in co-culture with MC and EC, in order to further establish D-PHI's potential use in the construction of a peripheral artery vascular graft. D-PHI films were seeded with EC followed by MC in vitro allowing for measurements of cellular proliferation, enzymatic activity, and cytokine production.

In addition to establishing D-PHI's suitable properties in vitro with all three cell types (MC, VSMC, and EC), the next step in assessing the suitability of D-PHI for a vascular graft was to establish the nature of the acute foreign body reaction it may elicit upon implantation. In the other half of this study, the material in scaffold form (without seeded cells) was further analyzed in vivo using a subcutaneous implant on the dorsal surface of a mouse. Explanted scaffolds allowed for the assessment of a full cytokine profile as well as histological analysis which provided greater detail on the manner by which this material would integrate with host tissue.

MATERIALS AND METHODS

Unless specified otherwise all reagents were purchased from Sigma–Aldrich, St. Louis, MO.

POLYMER SYNTHESIS–FILMS AND SCAFFOLDS

All polymer synthesis was completed according to the procedure of Sharifpoor et al. (2009). Briefly, a divinyl oligomer (DVO) was synthesized by reacting hydroxyethylmethacrylate, polyhexamethylene carbonate diol, and lysine diisocyanate in a 2:1:2 ratio in dimethylacetamide with dibutyltin dilaurate as the catalyst. The D-PHI material was made by mixing DVO (acts as a cross-linker) with methacrylic acid (MAA) and methyl methacrylate (MMA) in a ratio of 1:5:15, respectively, in the presence of a benzoyl peroxide (BPO) initiator (0.0015 mol/mol vinyl group) for 18–24 h. In order to make the films, the mixture was cast in a 96 well polypropylene plate and cured at 110°C for 24 h in a nitrogen-filled oven. The films were then stored in the absence of light and prior to use were soaked in 70% ethanol for 3–5 h. Following this procedure, the films were transferred to a 96 well tissue culture polystyrene plate and hydrated overnight in phosphate buffered saline (PBS) with 4% penicillin/streptomycin prior to seeding with MC and/or EC (McBane et al., 2009a).

The same polymerization reaction was used to generate the scaffolds (75% porous). After the addition of BPO initiator, the resulting blend was allowed to mix for a minimum of 12 h (room temperature, light protected) prior to the addition of $NaHCO_3$ particles (65 wt% relative to resin; 95 wt% of particles were in the range of 105–420 μm). Following an additional 12 h of mixing (room temperature, light protected) the final paste was loaded into Teflon molds (6 mm diameter, 2 mm thick) and cured at 110°C for 24 h. Upon the completion of the curing process, the disk-shaped

scaffolds were subjected to a 14-day salt leaching process with sonication in distilled water.

ISOLATION OF MONOCYTES

Human MC were isolated from 30 mL of blood donated from healthy volunteers and collected into ethylenediaminetetraacetic acid (EDTA)-containing Vacutainers (Becton Dickenson, Toronto, Canada) with approval of the Ottawa Hospital Research Ethics Board, Ottawa, Canada protocol# HI-2005979-01H as described in detail previously by (McBane et al., 2009a). The blood was layered onto 20 mL of Histopaque 1077 in a 50 mL polypropylene centrifuge tube (Falcon 2098). Centrifugation took place at 800 × *g*. The plasma layer was removed and the layer containing MCs was transferred to a new 50 mL Falcon tube where it was washed 5 times using 30 mL of wash buffer (282 mL RPMI media, 3 mL fetal bovine serum (FBS), 15 mL 6.5% EDTA) followed by centrifugation at 450 × *g* for 10 min per wash. After the final wash, the pellet was re-suspended in 10% (FBS media and counted in the automated Vicell™ Cell Viability Analyzer/Cell Counter (Beckman Coulter; Miami, FL).

CO-CULTURE OF ENDOTHELIAL CELLS AND MONOCYTES

Following thawing, human coronary artery ECs (HCAEC) (Lonza, cat. no. 2585, Walkersville, MD) were cultured in supplemented Clonetics® EC growth medium (EGM-2 MV)(Lonza, cat. no. 3202) in a 25 mL tissue culture flask until confluent (from 3 to 5 days). The ECs at confluence were passaged and then used for experiments between passages 2 and 4. ECs were seeded alone for 24 h following which MC (isolated as described above) were seeded either alone or in a 3:1 ratio of MC/EC (approximately 30,000:10,000 cells). These cell numbers were based on previous studies where MC were cultured alone on D-PHI (McBane et al., 2009a) or together with VSMC (McBane et al., 2011b) and were adjusted for the difference in the average cell diameter (MC 8–12 μm; EC 10–20 μm as determined by the Vicell™ Cell Viability Analyzer/Cell Counter (Data not shown)) and EC growth rate (MC do not divide). The co-culture and each individual cell culture (MC and EC alone) were then maintained with a 50:50 mixture of RPMI media and EGM-2 MV. The medium was changed 2 h after the MC were seeded and every 48 h onwards with 200 μL of media composed of 50% of RPMI media (10% FBS, 2% penicillin/streptomycin and 0.69 mM L-glutamine in RPMI with 12.7 mM HEPES) and 50% EGM-2 MV.

ASSAY OF ESTERASE ACTIVITY

Conditioned media (cell supernatant), that remained on the cells for 48 h prior to removal, and lysates were collected and assayed for esterase activity as described in detail previously by McBane et al. (2007). The substrate *p*-nitrophenylbutyrate (PNB) was used to define a unit of activity which is equal to the release of 1nmol of *p*-nitrophenol ($\epsilon = 16{,}300/cm/M$) per minute at 37°C at pH 7.0 at 400.6 nm over a 30 min incubation. The absorbance was read in a spectrophotometer (Beckman Model 640, Beckman Instruments, Richmond, CA.) and the activities were then normalized to 1 μg of protein.

ASSAY OF PROTEIN CONTENT

The amount of protein in the lysate obtained from each cell culture sample was assayed using the Bradford method (Bradford, 1976; Bradford reagent was obtained from Bio-Rad Laboratories Ltd., Mississauga, ON). Bovine serum albumin (BSA) was used to create a standard curve for which to compare the protein content of each sample.

SCANNING ELECTRON MICROSCOPY

Cells cultured on the D-PHI films in vitro and the explanted scaffolds, after 2 weeks in vivo, were fixed in 3% glutaraldehyde in PBS and then stored at 4°C prior to SEM analysis as described in detail previously (McBane et al., 2005). They were then dehydrated with increasing concentration of ethanol (30%, 50%, 70%, 90%, 95%, and 100% for 1 h each) before critical point drying, mounting on stubs, and platinum coating. The samples were photographed in the Faculty of Dentistry at the University of Toronto using a Hitachi S 2500 Scanning Electron Microscope (Hitachi, Mito City, Japan) with an operating voltage of 10 kV.

IMMUNOBLOTTING ANALYSIS OF CD31

Samples were loaded based on protein values determined using the Bradford method as previously described (Matheson et al., 2002). SDS-PAGE gels used for immunoblotting analysis were transferred to a BioTRace nitrocellulose membrane (VWR, Mississauga, ON), followed by blocking in a 5% BSA solution in TBS-Tween20, and incubation with mouse anti-human CD31 (R&D Systems; 1:200 in 1% BSA; Cedarlane Laboratories, Burlington, ON) overnight at 4°C. Blots were washed and incubated with secondary goat anti-mouse immuno-globulin G antibody conjugated to horseradish peroxidase (Pierce Chemical Co., Gilbertsville, PA) at 1:2500 in 5% BSA). Protein bands were visualized with an enhanced chemiluminescence detection system (SuperSignal West Pico; Thermo Scientific, Ottawa, ON) and recorded on Kodak X-ray film (Thermo Scientific).

ASSAY OF GROWTH WITH WST

The cell proliferation reagent, WST-1, (water-soluble tetrazolium-1; Cat no. 05015944001) (ROCHE Canada, Missisauga, ON) was used to measure cell activity and growth at 2, 4, and 7 days. Ten microliters of WST-1 and 90 μL of media were added to each well and left to incubate until a color change was observed. Plates were read in a microplate reader (Bio-Rad Model 3550-UV, GMI, Inc., Ramsey, MN) at an absorbance of 450 nm and background measured at 690 nm was subtracted. Data were normalized to absorbance (optical density (OD)/hour).

ASSAY OF CYTOKINES BY ELISA

ELISAs for TNF-α (eBioscience, Ready-Set-Go Cat no. 88-7346-88 and IL-10 Cat no. 88-7106-88; eBioscience, San Diego, CA) were carried out according to the protocol and the certificate of analysis supplied by the manufacturer in each kit. Costar 9018 high binding capacity plates (eBioscience) were coated with capture antibody in coating buffer overnight at 4°C. Plates were then washed and

blocked with assay diluent. Standards supplied in the kit were used to create the standard curve and 100 μL of sample were placed in each well. Samples were left to incubate overnight at 4°C. Plates were washed the following day and then detection antibody was added for 1 h followed by another series of washes. Avidin-HRP was then added for 30 min followed by washes and the addition of substrate solution for 15 min. Stop solution consisting of 2 N sulfuric acid was then added before the plates were read at 450 nm in a microplate reader (Bio-Rad Model 3550-UV, GMI, Inc.).

IN VIVO SURGERY/SCAFFOLD PREPARATION

BALB/c mice (female, ~20 g, 4–6 weeks) (Charles River) were anaesthetized with isoflurane and two scaffolds/mouse (without seeded cells) were placed in subcutaneous pockets on the dorsal surface of the animal and the incision closed with sutures (7-0 silk) (approval by the Animal Care Veterinary Service Committee, University of Ottawa, Ottawa, ON, protocol number H-248). Prior to the implantation of scaffolds, they were treated with a 70% ethanol solution overnight and then left in sterile filtered PBS containing 4% penicillin/streptomycin. Three mice were used at each time point (1 day, 1, 2, 4, and 6 week). At the time of explantation, the scaffolds were removed and placed in cold PBS on ice. For histological analysis, a 1 week scaffold sample was fixed in 4% paraformaldehyde for 25 min before being dehydrated in consecutive solutions of 15% and 30% sucrose. Following the dehydration procedure, this scaffold was sliced (Cryostat, Leica CM3050S) into 25 μm thick slices after being embedded in optimal cutting temperature (OCT) compound (Tissue-Tek, Sakura). Slices were placed on Superfrost Plus White pre-cleaned $25 \times 75 \times 1\ mm^3$ micro slides (VWR Micro Slides) prior to staining for histological analysis. Another scaffold explanted after 2 weeks was fixed in 3% glutaraldehyde for SEMs and processed as described above. Additional scaffolds were also implanted in mice for 1 week in order to examine acute viability using a live/dead assay described in detail below.

CYTOKINE ANTIBODY ARRAY

RayBio mouse cytokine antibody arrays (RayBiotech, Inc., Norcross, GA, Cat# AAM-CYT-1) were utilized in order to assess the amount of cytokines present in the explanted scaffolds. The explanted scaffolds were frozen at each time point (1 day to 6 weeks) and stored at −80 °C until analysis. After thawing on ice, 2 mL of cell lysis buffer (supplied with the array kit) was added to the scaffold prior to homogenization in a hand held Dounce homogenizer. Protease inhibitor cocktail (Cat. no. 8340, Sigma–Aldrich) was added to each sample in a ratio of 1:200 according to the supplier's instructions. Bradford assays were performed to assay protein levels in the homogenates, and cytokine antibody membranes were incubated with 250 μg of lysate protein according to the manufacturer's protocol. Detection took place in a chemiluminescence imaging system (FluorChemHD, Alpha Innotech, Cell Biosciences, Santa Clara, CA). The quantification of each image was carried out by AlphaEaseFC software. All cytokines assessed were normalized to their values at day 1 after normalizing all values on the arrays to an internal positive control provided by the manufacturer.

HISTOLOGICAL ANALYSIS

MASSON-TRICHROME STAINS

Following the slicing using a cryostat as described above, and removal of OCT from the explanted scaffolds with PBS, Masson-Trichrome (Sigma–Aldrich) staining was used to distinguish connective tissue, muscle, and collagen fibers using the protocol supplied by the supplier. Briefly, the slices were placed in preheated Bouin's Solution (HT10-1) at 56°C for 15 min then allowed to cool in tap water at room temperature. The slides were then washed in tap water and stained in Weigert's Iron Hematoxylin solution for 5 min followed by a second wash in tap water and then a rinse in deionized water. The Biebrich Scarlet-Acid Fuschin Stain (HT15-1) was then placed on the slides for 5 min followed by another rinse in deionized water. A solution of phosphotungstic/phosphomolybdic (1:1 v/v) acid in 2 volumes of deionized water was then placed on the slides for 5 min at which point the slides were transferred to an aniline blue solution (HT15-4) for 5 min and a 1% acetic acid solution for 2 min. Slides were then rinsed and dried. Images were photographed using a Leica DFC 420 CCD camera mounted on a light microscope (LEICA DM2500) operated by Image-Pro 6.2 software.

MAY-GRUNWALD GIEMSA STAIN

The May-Grunwald Giemsa stain (Sigma–Aldrich) was used to distinguish various cell types present in scaffold sections. The Giemsa stain was diluted 1:20 with deionized water before the slides were placed in the May-Grunwald stain for 5 min. They were then transferred to PBS, pH 7.2 for 90 s, followed by treatment with dilute Giemsa solution for 15–20 min. The slides were briefly rinsed in deionized water, observed, and photographed as described above.

LIVE/DEAD ASSAY

A live/dead assay was performed according to the procedure of Thevenot and Tang (2007). Stock solutions were prepared for carboxylfluorescein diacetate, succinimidyl ester (CFDA-SE, 5 mM in dimethylsulfoxide) and propidium iodide (PI, 1.5 mM in deionized water; Invitrogen Canada, Burlington, ON). The explanted scaffolds were rinsed in PBS and then immersed in CFDA-SE (final concentration 2.5 μM in PBS) reagent for 20 min at 37°C. Following this, the scaffolds were fixed in methanol for 10 min and stained with PI (500 nM in 2x SSC [0.3 M NaCl, 0.03 M sodium citrate, pH 7.0]) for 5 min. The scaffolds were washed briefly in PBS and frozen. After imbedding in OCT and sliced as described above, the sections were examined using an Olympus IX80 laser scanning confocal microscope operated by FV1000 software v1.4a.

STATISTICAL ANALYSIS

Statistical analysis was performed with ANOVA using SAS 9.2 with significance reported for $P < 0.05$. All data ($n = 3$) were plotted with standard error of the mean (SE).

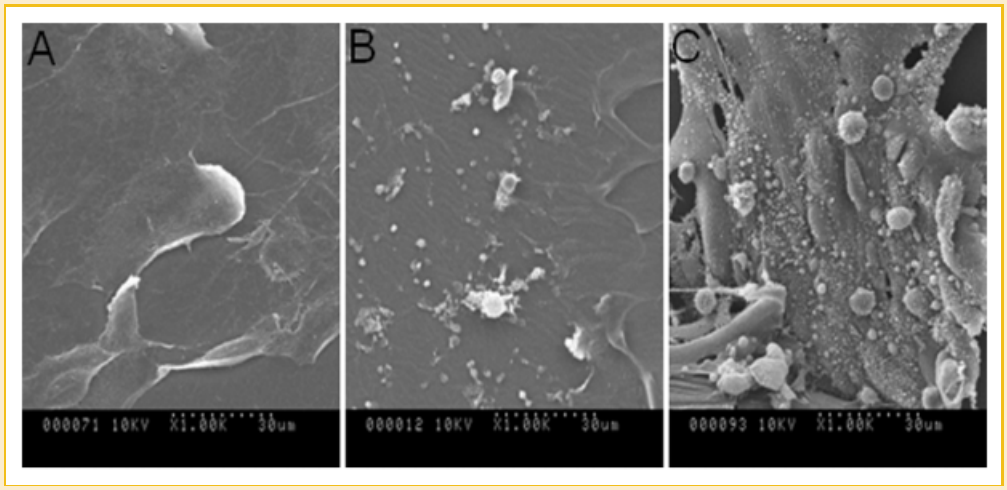

Fig. 1. Scanning electron microscopy (SEM) of EC, MC and the co-culture on D-PHI. EC (A), MC (B), and both EC and MC (C) were cultured on D-PHI for 48 h and fixed for SEM. Magnification 1,000x, scale bar 30 μm.

RESULTS AND DISCUSSION

In order to establish a successful co-culture of ECs and MC on D-PHI prior to the development of functional assays, the ratio, and number of the two cell types seeded was investigated. The influence of D-PHI on differentiating MC and EC separately and together was assessed through the measurement of cell attachment using DNA analysis which has been shown previously to correlate with attachment and viability (McBane et al., 2009b) as well as EC metabolic growth determined with WST. After testing different combinations of media it was determined that a 50:50 mixture containing the media of preference for each cell type (MCs, RPMI, and the media of preference for the EC, EGM-2MV), was adequate to grow both cell types in co-culture.

SEMs (Fig. 1) taken 48 h after the seeding of EC alone (Fig. 1A), MC alone (Fig. 1B) and the co-culture (Fig. 1C) make it apparent that the two cell types survived alone and together on D-PHI. EC alone as well as in the co-culture were able to form a monolayer (Fig. 1A,C), which was suggestive of a highly functional phenotype. In addition, the cells in the co-culture appeared to remain viable while in close contact with one another and maintained their typical morphology (Fig. 1C).

When a proliferation assay was conducted the co-culture did not show a significant difference when compared to EC alone, Figure 2 shows that D-PHI allowed for good cell adhesion and viability with a significant increase in proliferation of EC during the 1 week culture period (~13 fold; $P < 0.05$). MC mitochondrial activity remained constant over the 2, 4, and 7 day time points since MC/MDM do not proliferate (Papadimitriou and Ashman, 1989).

A noteworthy finding of the in vitro studies was established through immunoblotting analysis, which showed that the EC maintained their CD31 marker when cultured alone and in co-culture with MC on D-PHI (Fig. 3). As anticipated no CD31 was detectable in the MC culture alone. Since CD31 is indicative of adherent, functional ECs which have formed a confluent layer (Dvorin et al., 2003) the data suggest that culturing ECs with MC on D-PHI had no negative effect on EC maturation. When loading SDS-PAGE by equal amounts of protein, it appeared that CD31 was increased in the co-culture. However, it was not possible to find a suitable loading control that would allow quantification of CD31 in the EC and the co-culture simultaneously. The amount of GAPDH in MC was significantly different from EC and in addition varied greatly over the culture period as a percent of total cell protein between the MC which did not divide versus EC which did (Data not shown).

A recent study showed that mature human EC could modulate endothelial progenitor cells (EPC) in the MC fraction isolated from human donors when seeded on fibronectin and cultured in EBM-2 medium (Bellik et al., 2008). The co-culture in this case did not involve cell to cell contact but shared the same culture medium. Although many EC markers were expressed on the differentiating

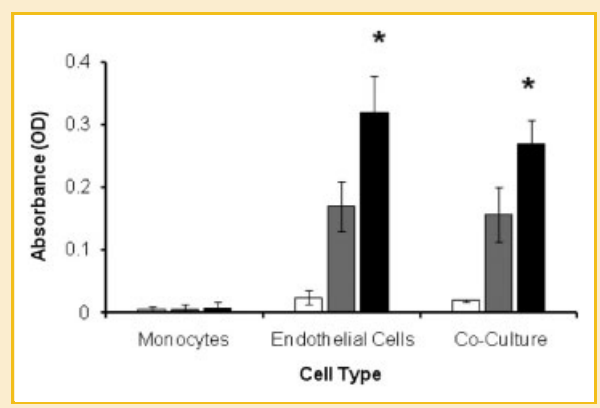

Fig. 2. Assay for the growth of MC, EC, and the co-culture on D-PHI. The growth of MC, EC, and the co-culture on D-PHI at 48 h (white), 96 h (gray), and 7 days (black) was determined using a WST assay. Optical density (OD) is proportional to cell proliferation and activity is shown for each set of culture conditions. Growth increased significantly in EC culture and co-culture between all time points $^{*}P = < 0.05$ ($n = 3 \pm SE$).

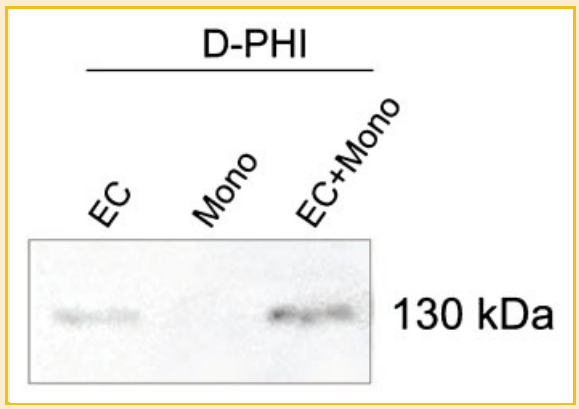

Fig. 3. Immunoblotting analysis of the expression of CD31 in the MC, EC, and co-culture. Immunoblotting analysis was performed on cell lysates using an antibody to CD31 after 7 days in culture on D-PHI.

EPC, CD 31 was not detected. In the current study, an important finding was that the CD31 expressed in the co-culture was due only to the EC and not the MC. When the conditioned medium which was removed from ECs cultured for 1 week in EGM-2MV and was added to MC cultured alone, no CD31 expression was detected in the 7 day old MC (Data not shown). This showed that MC were able to maintain their phenotype when exposed to signals released into the local cellular environment by EC (Dvorin et al., 2003).

Esterase activity in MC/MDM has been shown to be linked to the degradation of biomaterials and has been used as a marker of degradative potential (Labow et al., 2001). Figure 4 shows the changes in esterase activity normalized to protein in cells cultured on D-PHI for 48 h and 7 days. In order to compare the total esterase activity in the co-culture to each cell's activity cultured alone, the data in Figure 4 were presented as stacked bars. There was significantly more esterase activity when the EC and MC esterase activity was added together for the cells cultured individually at 7 days as compared to the co-culture ($P = 0.04$). When EC were cultured alone, there was a significant increase in the esterase activity at 7 days (~30%, $P < 0.05$) whereas such an increase was not seen in the co-culture. As was previously found with MC cultured alone on D-PHI (McBane et al., 2009a), the esterase activity did not increase significantly over the course of the week. By culturing EC with MC, the total esterase activity was significantly reduced indicating that the cells experienced reduced activation in co-culture. While esterase activity may not be traditionally associated with ECs, non-specific esterase activities have been found in the Weibel-Palade bodies, on the external surface of the plasma membrane and on cytoplasmic lipid bodies in aortic ECs (Monahan-Earley et al., 1987). And although it is esterase activity that has been shown to be the most degradative to polyurethanes (Santerre et al., 2005), the esterolytic activity of serine proteases (which exist in all cell types) has been shown to have some degradative potential (Labow et al., 1999). The reduced esterase activity in co-culture, in addition to demonstrating reduced activation, also suggests (which has recently been shown in a rat in vivo model McBane et al., 2011a), that the material, once implanted, would not undergo immediate hydrolytic degradation, a quality that is important in maintaining scaffold form and structure for a vascular graft until repopulation of the graft with appropriate cells occurs (Conklin et al., 2002; L'Heureux et al., 2006).

ELISAs for TNF-α and IL-10 were conducted on the conditioned media from MC, EC, and the co-culture grown on D-PHI films (Fig. 5). Although not significantly different, there was a consistent observation of yielding higher levels of IL-10 relative to the levels of TNF-α, and both cytokines decreased over time. An important finding was that no TNF-α could be measured in the co-culture by 7 days, although IL-10 was still present. Not surprising, ECs alone showed virtually no cytokines while the levels in MCs alone were high. While TNF-α is associated with the inflammatory response,

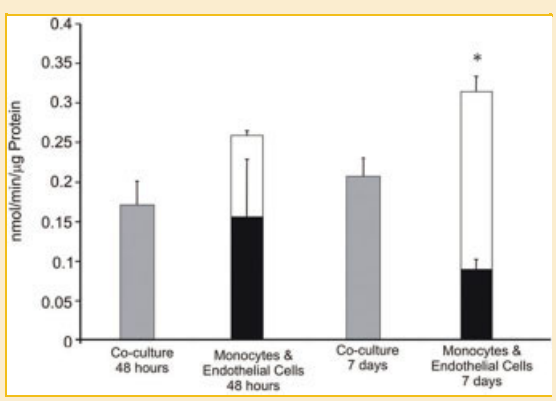

Fig. 4. Esterase activity in MC, EC, and the co-culture on D-PHI. Esterase activity (nmol/min/μg protein) in cell lysates was assayed at 48 h and 7 days for each surface (monocytes (black); ECs (white); co-culture (gray)) ($n = 3 \pm$ SE) (*significantly more esterase activity when the activity of MC and EC cultured separately was added together and compared to the co-culture ($P = 0.04$).

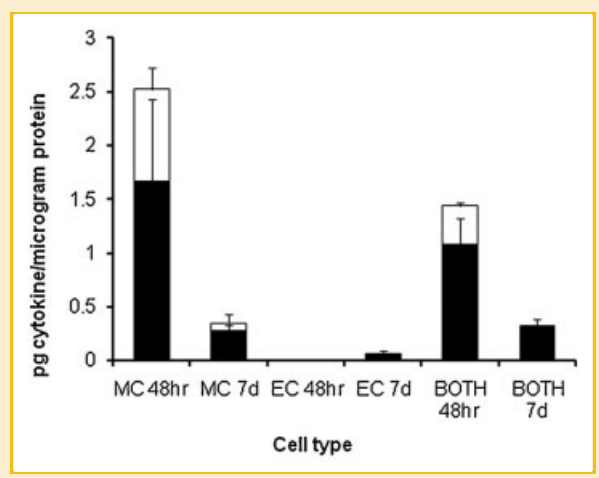

Fig. 5. Cytokine analysis by ELISA for conditioned media of MC, EC, and the co-culture on D-PHI. TNF-α (white) and IL-10 (black) present in the MC, EC, and co-culture conditioned medium was normalized to protein at 48 h and 7 days and assayed by ELISA. While the levels of both cytokines decreased over time, the inflammatory cytokine TNF-α was no longer present by day 7 in the co-culture. ($n = 3 \pm$ SE).

IL-10 is considered anti-inflammatory (Schutte et al., 2009). A previous study has shown that IL-10 has anti-inflammatory effects on MC/endothelium interactions and may actually be produced as a result of these interactions (Noble et al., 2000; Mostafa Mtairag et al., 2001).

Since the three cell types that inevitably will be involved in the regeneration of a vascular graft (MC, VSMC, and EC; Kakisis et al., 2005), responded favorably in vitro when cultured on D-PHI in this study with ECs and in previous studies with VSMCs (McBane et al., 2011b), by eliciting an anti-inflammatory reaction, it was of interest to assess the in vivo response. D-PHI was assessed for its foreign body reaction (without seeded cells) in vivo. Three-dimensional porous scaffolds were prepared from D-PHI as described above and implanted in the subcutaneous mouse model. Figure 6 shows a SEM image of a D-PHI scaffold that was explanted from a BALB/c mouse following a 2 week subcutaneous implant showing that cells and extracellular matrix were adherent to the scaffold (Panel A). Vascularization may also have occurred since it appears that it might be a vessel growing over the surface of this scaffold (B). Panel (C) shows a control scaffold, which was not implanted for comparison purposes.

The live/dead assay indicated that the cells were viable within the scaffolds (Fig. 7A–D). A green stain indicates live cell cytoplasm (Panel A) while red stains indicate nuclei (Panel B). Red nuclei that were not surrounded by green cytoplasm would indicate dead cells. However, none were visible indicating that the cells within the scaffolds were viable (Panel C, overlay). Panel D was a cross-section half way through the scaffold and shows that cells have migrated into the pores of the structure while maintaining their viability.

The histological analysis confirmed the results of the SEM images. Figure 7E–H shows the results for the tissue in-growth (extracellular matrix, cells). Panels (E) and (G) show the results of the May-Grunwald Giemsa stain on the explanted scaffold while (F) and (H) show the scaffold that was not implanted. In panel (E) the edge of the scaffold is visible and tissue migration into the scaffold and surrounding the scaffold may be observed. Panel (G) shows tissue formation inside of the scaffold. Blue/pink staining reveals cell cytoplasm while the nuclei are varying shades of purple. The May-Grunwald Giemsa stain has been used by others to demonstrate the differences in cell attachment to polyurethanes that differed in material surface chemistry (Christenson et al., 2004). The findings confirm that within 2 weeks, tissue integration within the scaffold was extensive.

The Masson-Trichrome stain (Fig. 7I–L) showed the presence of collagen and muscle fibers in addition to cells. This stain has been used extensively to show tissue in growth in synthetic vascular grafts (Fujimoto et al., 1993; Amabile et al., 2002). The deposition of collagen can be observed surrounding the scaffold in panel (I) and migrating into the scaffold in panel (K) while panels (J) and (L) show the background stain from the scaffold alone in the absence of implantation. Nuclei stain black and cytoplasm stains red allowing for the detection of cells within the extracellular matrix. Both May-Grunwald Giemsa and Masson-Trichrome stains provided evidence that excellent tissue in-growth occurred in the implanted scaffolds while maintaining cell viability as demonstrated by the live/dead assay (Fig. 7A–D).

The in vivo results generated from the cytokine antibody array for protein analysis within the explanted scaffolds (Fig. 8) confirm the results obtained in vitro with the ELISAs (Fig. 5). The profile of the cytokines produced by cells in the local tissue and/or those which migrated into the scaffold following implantation generally supported the concept of a low inflammatory mechanism in the foreign body response to D-PHI.

The data in Figure 8A for MCP-1 and MCP-5 show that MCP-5 was significantly higher at 1 week, whereas MCP-1 was significantly higher at 6 weeks relative to other time points. It has been shown that MCP-1 significantly increases the level of perfusion in an ischemic porcine hindlimb (Voskuil et al., 2003). Increased MCP-1 levels have also been correlated with the invasion of VSMCs (Wang et al., 2011), a population of cells previously noted for its extensive compatibility with D-PHI and importance in the generation of a vascular graft. The fact that these chemokines were elevated may be

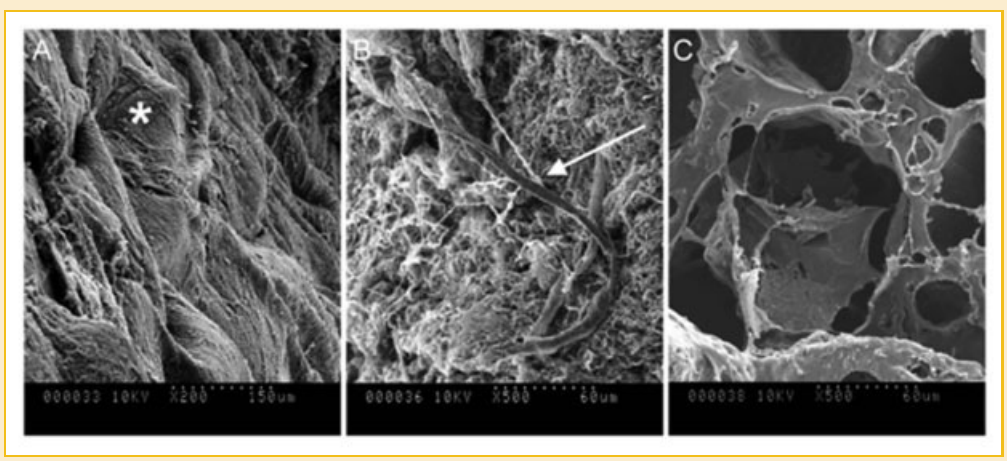

Fig. 6. Scanning electron microscopy (SEM) of an explanted scaffold following a 14 day subcutaneous implant period in the mouse (A) and (B) and a control scaffold not implanted (C). Note the deposition of extracellular matrix in (A) (*) (200x magnification) and a blood vessel growing on the surface of the explanted scaffold (B) (arrow) (500x magnification; scale bar (A) 150 μm; scale bar (B) and (C) 60 μm).

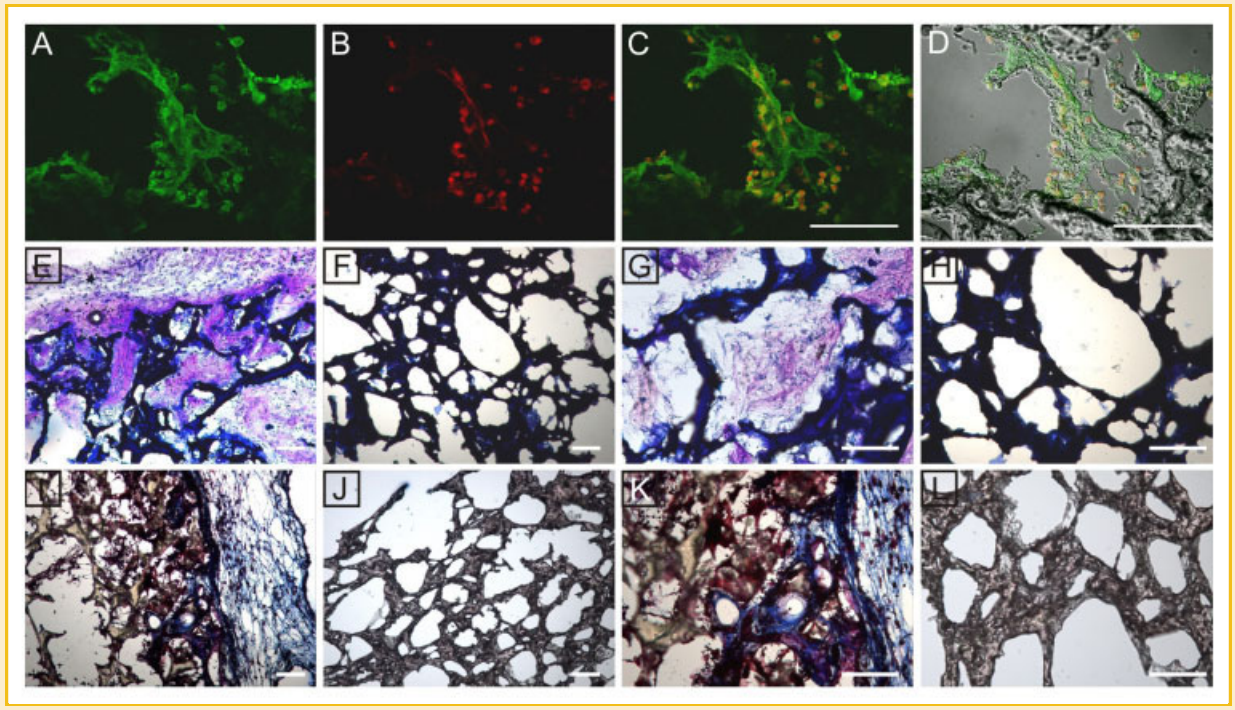

Fig. 7. Histological assessment of explanted scaffolds for cell viability and tissue in growth. A live-dead fixed assay (Panels A–D) shows the cytoplasm of live cells stained green (A), nuclei stained red (B), overlay (C), and phase contrast (D). Histological staining with May-Grunwald Giemsa is shown in Panels (E–H). (E) and (G) show the explanted scaffold. Panels (F) and (H) show the scaffold which was not implanted. Panels (I–L) show the Masson-Trichrome stain (J and L, scaffold not implanted; scale bar = 100 μm). [Color figure can be seen in the online version of this article, available at http://wileyonlinelibrary.com/journal/jcb]

beneficial in that increased MC recruitment to the D-PHI scaffold would allow for establishing a wound healing phenotype MDM. Increased secretion of anti-inflammatory/pro-wound healing chemokines would aid in vascular tissue regeneration (Roh et al., 2010). Based on the above in vitro studies of EC and MC (no TNF-α at 7 days; Fig. 5) and in previous in vitro studies of MC data with (McBane et al., 2011b) or without (McBane et al., 2009a) VSMC, it was found that MC adhere to D-PHI and differentiate to a wound healing MDM.

IL-12 is a pivotal cytokine that links the innate and adaptive immune responses. TNF-α is a potent inhibitor of IL-12 p40 and IL-12p70 secretion from human macrophages induced by lipopolysaccaride (LPS) or *Staphylococcus aureus* identifying a direct negative feedback mechanism for inflammation-induced suppression of IL-12 gene expression. The reciprocal influence of these two inflammatory mediators on each other may have a significant impact on the cytokine balance that shapes the type and extent of immune responses (Ma et al., 2000). The cytokine array measured the ratio of IL-12p40 to IL-12p70. IL-12p40 monomers and homodimers can bind the IL-12 receptor without triggering cell signaling (Ling et al., 1995). Therefore this ratio represents the inactive (p40) versus the pro-inflammatory (p70) subunits of IL-12 and a high ratio leads to decreased inflammation (Piazzolla et al., 2001). The increased level of IL-12p40/p70 at 4 and 6 weeks (Fig. 8B) may therefore be a beneficial response to D-PHI.

Granulocyte/macrophage colony stimulating factor (GM-CSF) peaked at 1 week which was significantly greater than at 1 day (Fig. 8C). GM-CSF has the ability to stimulate the differentiation and function of granulocytes, MC, and macrophages (Esen and Kielian, 2007), which is desirable at an early time. Furthermore, GM-CSF-induction has also been shown to increase the transcription of MCP-1 and the infiltration of MDM, both of which are important features for tissue engineering of vascular grafts (Maekawa et al., 2004). Again, D-PHI's chemistry should direct the differentiation to a wound healing phenotype as the time of implantation increases.

What is of considerable importance are the data reported for IL-6 (Fig. 8D). There were significantly higher levels of IL-6 at 1 day which subsequently decreased dramatically. IL-6 is produced at the site of inflammation and has an important role in the acute phase of inflammation as well as stimulating chronic inflammation (Gabay, 2006). The fact that it decreased over time showed that D-PHI would not result in chronic inflammation at the site of the implant.

The level of RANTES (Regulated on Activation Normal T cell Expressed and Secreted) showed a trend toward increasing over time with significantly more present at 4 and 6 weeks (Fig. 8E). RANTES could be considered a pro-inflammatory chemokine which promotes the accumulation and activation of cells during inflammatory conditions. However, recently it has been shown to recruit cells for angiogenesis and so in the long term it may be important for the vascularization of a D-PHI vascular graft (Westerweel et al., 2008).

The results presented for TNF-α (Fig. 8F) and IL-10 (Fig. 8G) clearly link the in vitro with the in vivo studies, supporting D-PHI as a material that elicits an anti-inflammatory response. TNF-α is considered a major mediator of inflammation and mediates diseases ranging from cancer, to arthritis to atherosclerosis through its ability to activate the transcription factor NF-κB (Aggarwal et al., 2002). In

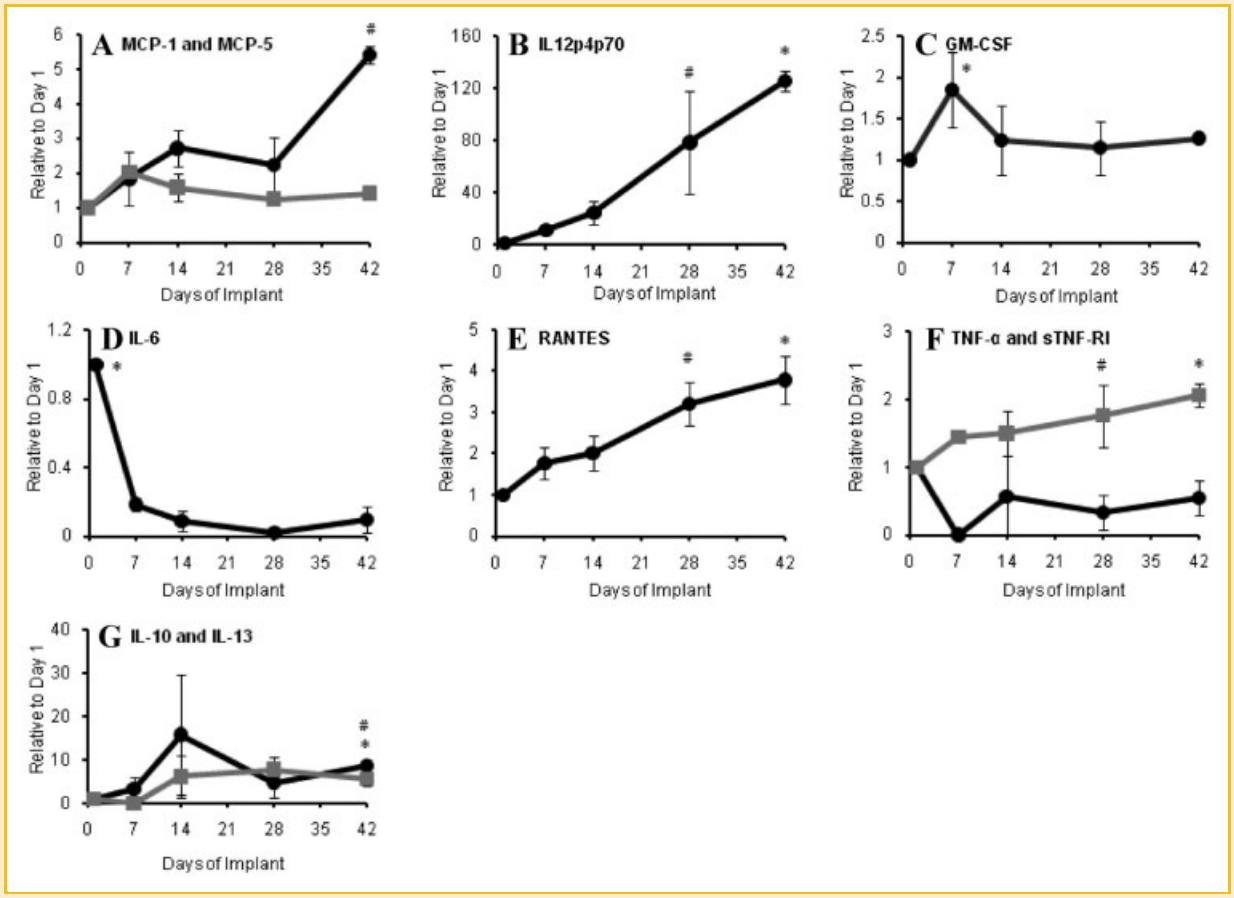

Fig. 8. Cytokine antibody array of lysate from explanted scaffolds. Each cytokine was normalized to the internal control supplied by the manufacturer and then calculated as a ratio to the respective value at day 1 which was set equal to 1. The data were plotted against the time the scaffold was implanted in days. A: Levels of MCP-5 and MCP-1. MCP-5 (gray square) was significantly higher at 7 days as compared to 1 day, 28 days, and 42 days ($^{*}P = 0.0013, 0.0075, 0.0266$). MCP-1 (black circle) was significantly higher at 42 days as compared to all of the other time points ($\#P < 0.0001, 0.0003, 0.0021, 0.0006$) ($n = 3 \pm SE$). B: Levels of IL-12p40p70. IL-12p40p70 levels were significantly higher at 28 ($\#P = 0.0044, 0.0098, 0.0286$) and 42 days ($^{*}P = 0.0002, 0.0003, 0.0007, 0.0491$) than at the other time points ($n = 3 \pm SE$). C: Levels of GM-CSF. GM-CSF was significantly higher than 1 day after 7 days ($^{*}P = 0.0410$) ($n = 3 \pm SE$). D: Levels of IL-6. IL-6 was significantly higher at 1 day than at any other time point ($^{*}P < 0.0001$) ($n = 3 \pm SE$). E: Levels of RANTES. RANTES was significantly higher at 28 ($\#P = 0.0013, 0.016, 0.0374$) and 42 days ($^{*}P = 0.0002, 0.0023, 0.0053$) than any at other time point ($n = 3 \pm SE$). F: Levels of TNF-α and sTNF-RI. TNF-α (black circle) did not change significantly during 42 days whereas sTNF-RI (gray square) was significantly higher than 1 day by 4 (#p= 0.0337) and 42 days ($^{*}P = 0.0063$; $n = 3 \pm SE$). G: Levels of IL-10 and IL-13). IL-10 (black circle) ($^{*}P = 0.0021$) and IL-13 (gray square ($\#P = 0.0357$) were both significantly higher by 42 days as compared to 1 day. ($n = 3 \pm SE$).

this study, TNF-α levels were not significantly higher after D-PHI was implanted for 6 weeks than at day 1. Moreover, the level of sTNF-receptor (R) I was significantly greater at the 4 and 6 week time points than at any other time point. Studies have shown that sTNF-RI is part of an anti-inflammatory pathway whereby it signals a protective mechanism to tissues from disease (Williams-Skipp et al., 2009), so although TNF-α did not change over time, TNF-RI went up significantly. The results for IL-10 and IL-13 further complemented and confirmed the data that D-PHI promotes an anti-inflammatory response. IL-10 has been shown to regulate activated macrophages and antigen-presenting cells through decreasing cytokine and chemokine production from macrophages and dendritic cells, ultimately limiting chronic and acute inflammation (Murray, 2005). Although less potent than IL-10, IL-13 has been shown to have similar abilities to IL-10 in down regulating an inflammatory response (Marie et al., 1996). Both of these anti-inflammatory cytokines went up significantly by 6 weeks relative to day 1 resulting in a higher IL-10 to TNF-α ratio at 6 weeks than at day 1, almost exactly what was found at 1 week in the in vitro studies with the co-culture, except that at 1 week no TNF-α could be detected (Fig. 5).

Although there were some cytokines released that under certain conditions would be considered pro-inflammatory, when summarizing the array profile, the data support an anti-inflammatory response overall.

In summary, this study has demonstrated that the D-PHI material, whether in film (in vitro) or scaffold (in vivo) form, invoked a response which included low levels of inflammation markers while allowing for cell viability and growth. In vitro, the co-culture of MCs with ECs on D-PHI films promoted a functional EC layer (CD31 expression) and significant EC growth relative to EC alone. Both in vivo and in vitro the ratio of IL-10 to TNF-α increased over time, supporting an anti-inflammatory response. While the anti-inflammatory cytokine IL-10 was released in the in vitro co-culture at 7

days, there was no detectable pro-inflammatory cytokine TNF-α at that time. A similar pattern was observed in vivo. IL-10 was significantly higher by 6 weeks in vivo whereas TNF-α levels remained relatively constant. A live/dead assay indicated that the cells that had migrated into the scaffold were viable, while histological analysis showed tissue integration with extracellular matrix formation. Therefore, the results of this study indicate that D-PHI promoted wound healing MC and functional EC growth in co-culture, while eliciting an anti-inflammatory response from cells both in vitro and in vivo.

ACKNOWLEDGMENTS

This study was funded by a Collaborate Health Research Program grant (CHRP #337246). Sarah McDonald was funded by an Ontario Graduate Scholarship, Loren Matheson by a Canadian Arthritis Network post-doctoral fellowship, Joanne McBane by a Heart and Stroke Foundation Fellowship (Focus on Stroke VII) and Drew Kuraitis by a Heart and Stroke Foundation Ontario Master's Studentship Award. The authors thank Kelsey Santerre for her technical assistance in the in vitro studies, Branka Vulesevic for her technical assistance in the in vivo studies and Soroor Sharifpoor for advice on the D-PHI synthesis.

REFERENCES

Aggarwal BB, Shishodia S, Ashikawa K, Bharti AC. 2002. The role of TNF and its family members in inflammation and cancer: Lessons from gene deletion. Curr Drug Targets 1(4):327–341.

Amabile PG, Wong H, Uy M, Boroumand S, Elkins CJ, Yuksel E, Waugh JM, Dake MD. 2002. In vivo vascular engineering of vein grafts: Directed migration of smooth muscle cells by perivascular release of elastase limits neointimal proliferation. J Vasc Interv Radiol 13(7):709–715.

Anderson JM, Rodriguez A, Chang DT. 2008. Foreign body reaction to biomaterials. Semin Immunol 20(2):86–100.

Bellik L, Musilli C, Vinci MC, Ledda F, Parenti A. 2008. Human mature endothelial cells modulate peripheral blood mononuclear cell differentiation toward an endothelial phenotype. Exp Cell Res 314(16):2965–2974.

Bonfield TL, Colton E, Anderson JM. 1989. Plasma protein adsorbed biomedical polymers: Activation of human monocytes and induction of interleukin 1. J Biomed Mater Res 23(6):535–548.

Bradford MM. 1976. A rapid and sensitive method for the quantitation of microgram quantities of protein utilizing the principle of protein-dye binding. Anal Biochem 72:248–254.

Christenson EM, Dadsetan M, Wiggins M, Anderson JM, Hiltner A. 2004. Poly(carbonate urethane) and poly(ether urethane) biodegradation: In vivo studies. J Biomed Mater Res 69A(3):407–416.

Conklin BS, Richter ER, Kreutziger KL, Zhong DS, Chen C. 2002. Development and evaluation of a novel decellularized vascular xenograft. Med Eng Phys 24(3):173–183.

Dvorin EL, Wylie-Sears J, Kaushal S, Martin DP, Bischoff J. 2003. Quantitative evaluation of endothelial progenitors and cardiac valve endothelial cells: Proliferation and differentiation on poly-glycolic acid/poly-4-hydroxybutyrate scaffold in response to vascular endothelial growth factor and transforming growth factor beta1. Tissue Eng 9(3):487–493.

Esen N, Kielian T. 2007. Effects of low dose GM-CSF on microglial inflammatory profiles to diverse pathogen-associated molecular patterns (PAMPs). J Neuroinflamm 4:10.

Fujimoto K, Inoue H, Ikada Y. 1993. Protein adsorption and platelet adhesion onto polyurethane grafted with methoxy-poly(ethylene glycol) methacrylate by plasma technique. J Biomed Mater Res 27(12):1559–1567.

Gabay C. 2006. Interleukin-6 and chronic inflammation. Arthritis Res Ther 8(Suppl 2):S3.

Goodney PP, Beck AW, Nagle J, Welch HG, Zwolak RM. 2009. National trends in lower extremity bypass surgery, endovascular interventions, and major amputations. J Vasc Surg 50(1):54–60.

Kakisis JD, Liapis CD, Breuer C, Sumpio BE. 2005. Artificial blood vessel: The Holy Grail of peripheral vascular surgery. J Vasc Surg 41(2):349–354.

Konig G, McAllister TN, Dusserre N, Garrido SA, Iyican C, Marini A, Fiorillo A, Avila H, Wystrychowski W, Zagalski K, Maruszewski M, Jones AL, Cierpka L, de la Fuente LM, L'Heureux N. 2009. Mechanical properties of completely autologous human tissue engineered blood vessels compared to human saphenous vein and mammary artery. Biomaterials 30(8):1542–1550.

Labow RS, Meek E, Santerre JP. 1999. The biodegradation of poly(urethane)s by the esterolytic activity of serine proteases and oxidative enzyme systems. J Biomater Sci Polym Ed 10(7):699–713.

Labow RS, Meek E, Santerre JP. 2001. Model systems to assess the destructive potential of human neutrophils and monocyte-derived macrophages during the acute and chronic phases of inflammation. J Biomed Mater Res 54(2):189–197.

L'Heureux N, Dusserre N, Konig G, Victor B, Keire P, Wight TN, Chronos NA, Kyles AE, Gregory CR, Hoyt G, Robbins RC, McAllister TN. 2006. Human tissue-engineered blood vessels for adult arterial revascularization. Nat Med 12(3):361–365.

Ling P, Gately MK, Gubler U, Stern AS, Lin P, Hollfelder K, Su C, Pan YC, Hakimi J. 1995. Human IL-12 p40 homodimer binds to the IL-12 receptor but does not mediate biologic activity. J Immunol 154(1):116–127.

Ma X, Sun J, Papasavvas E, Riemann H, Robertson S, Marshall J, Bailer RT, Moore A, Donnelly RP, Trinchieri G, Montaner LJ. 2000. Inhibition of IL-12 production in human monocyte-derived macrophages by TNF. J Immunol 164(4):1722–1729.

Maekawa Y, Anzai T, Yoshikawa T, Sugano Y, Mahara K, Kohno T, Takahashi T, Ogawa S. 2004. Effect of granulocyte-macrophage colony-stimulating factor inducer on left ventricular remodeling after acute myocardial infarction. J Am Coll Cardiol 44(7):1510–1520.

Marie C, Pitton C, Fitting C, Cavaillon JM. 1996. Regulation by anti-inflammatory cytokines (IL-4, IL-10, IL-13, TGFbeta) of interleukin-8 production by LPS- and/ or TNFalpha-activated human polymorphonuclear cells. Mediat Inflamm 5(5):334–340.

Matheson LA, Labow RS, Santerre JP. 2002. Biodegradation of polycarbonate-based polyurethanes by the human monocyte-derived macrophage and U937 cell systems. J Biomed Mater Res 61(4):505–513.

McBane JE, Santerre JP, Labow RS. 2005. The role of protein kinase C in the monocyte-derived macrophage mediated biodegradation of polycarbonate-based polyurethanes. J Biomed Mater Res 74A:1–11.

McBane JE, Santerre JP, Labow RS. 2007. The interaction between hydrolytic and oxidative pathways in macrophage-mediated polyurethane degradation. J Biomed Mater Res A 82(4):984–994.

McBane JE, Matheson LA, Sharifpoor S, Santerre JP, Labow RS. 2009a. Effect of polyurethane chemistry and protein coating on monocyte differentiation towards a wound healing phenotype macrophage. Biomaterials 30(29):5497–5504.

McBane JE, Santerre JP, Labow R. 2009b. Effect of phorbol esters on the macrophage-mediated biodegradation of polyurethanes via protein kinase C activation and other pathways. J Biomater Sci Polym Ed 20(4):437–453.

McBane JE, Sharifpoor S, Cai K, Labow RS, Santerre JP. 2011a. Evaluating the biodegradation and in vivo biocompatility of a degradable, polar/ionic/polyurethane for tissue engineering applications. Biomaterials 32(26):6034–6044.

McBane JE, Battiston KG, Wadhwani A, Sharifpoor S, Labow RS, Santerre JP. 2011b. The effect of degradable polymer surfaces on co-cultures of monocytes and smooth muscle cells. Biomaterials 32(14):3584–3595.

Monahan-Earley RA, Isomura T, Garcia RI, Galli SJ, Dvorak HF, Dvorak AM. 1987. Nonspecific esterase activity expressed in Weibel-Palade bodies of cloned guinea pig aortic endothelial cells. J Histochem Cytochem 35(5):531–539.

Mostafa Mtairag E, Chollet-Martin S, Oudghiri M, Laquay N, Jacob MP, Michel JB, Feldman LJ. 2001. Effects of interleukin-10 on monocyte/endothelial cell adhesion and MMP-9/TIMP-1 secretion. Cardiovasc Res 49(4): 882–890.

Murray PJ. 2005. The primary mechanism of the IL-10-regulated antiinflammatory response is to selectively inhibit transcription. Proc Natl Acad Sci USA 102(24):8686–8691.

Noble KE, Harkness D, Yong KL. 2000. Interleukin 10 regulates cellular responses in monocyte/endothelial cell co-cultures. Br J Haematol 108(3): 497–504.

Papadimitriou JM, Ashman RB. 1989. Macrophages: Current views on their differentiation, structure, and function. Ultrastruct Pathol 13(4):343–372.

Piazzolla G, Tortorella C, Fiore G, Fanelli M, Pisconti A, Antonaci S. 2001. Interleukin-12 p40/p70 ratio and in vivo responsiveness to IFN-alpha treatment in chronic hepatitis C. J Interferon Cytokine Res 21(7):453–461.

Roh JD, Sawh-Martinez R, Brennan MP, Jay SM, Devine L, Rao DA, Yi T, Mirensky TL, Nalbandian A, Udelsman B, Hibino N, Shinoka T, Saltzman WM, Snyder E, Kyriakides TR, Pober JS, Breuer CK. 2010. Tissue-engineered vascular grafts transform into mature blood vessels via an inflammation-mediated process of vascular remodeling. Proc Natl Acad Sci USA 107(10): 4669–4674.

Santerre JP, Woodhouse K, Laroche G, Labow RS. 2005. Understanding the biodegradation of polyurethanes: From classical implants to tissue engineering materials. Biomaterials 26(35):7457–7470.

Schubert SY, Benarroch A, Ostvang J, Edelman ER. 2008. Regulation of endothelial cell proliferation by primary monocytes. Arterioscler Thromb Vasc Biol 28(1):97–104.

Schutte RJ, Parisi-Amon A, Reichert WM. 2009. Cytokine profiling using monocytes/macrophages cultured on common biomaterials with a range of surface chemistries. J Biomed Mater Res A 88(1):128–139.

Selvin E, Erlinger TP. 2004. Prevalence of and risk factors for peripheral arterial disease in the United States: Results from the National Health and Nutrition Examination Survey, 1999–2000. Circulation 110(6):738–743.

Sharifpoor S, Labow RS, Santerre JP. 2009. Synthesis and characterization of degradable polar hydrophobic ionic polyurethane scaffolds for vascular tissue engineering applications. Biomacromolecules 10(10):2729–2739.

Sharifpoor S, Simmons CA, Labow RS, Santerre JP. 2010. A study of vascular smooth muscle cell function under cyclic mechanical loading in a polyurethane scaffold with optimized porosity. Acta Biomater 6(11):4218–4228.

Stegemann JP, Nerem RM. 2003. Phenotype modulation in vascular tissue engineering using biochemical and mechanical stimulation. Ann Biomed Eng 31(4):391–402.

Thevenot P, Tang L. 2007. Novel method to monitor cell survival and distribution in a PLGA degradable scaffold. IEEE Xplore 54:39–42.

Voskuil M, van Royen N, Hoefer IE, Seidler R, Guth BD, Bode C, Schaper W, Piek JJ, Buschmann IR. 2003. Modulation of collateral artery growth in a porcine hindlimb ligation model using MCP-1. Am J Physiol Heart Circ Physiol 284(4):H1422–H1428.

Wang M, Spinetti G, Monticone RE, Zhang J, Wu J, Jiang L, Khazan B, Telljohann R, Lakatta EG. 2011. A local proinflammatory signalling loop facilitates adverse age-associated arterial remodeling. PloS One 6(2):e16653.

Westerweel PE, Rabelink TJ, Rookmaaker MB, Grone HJ, Verhaar MC. 2008. RANTES is required for ischaemia-induced angiogenesis, which may hamper RANTES-targeted anti-atherosclerotic therapy. Thromb Haemost 99(4):794–795.

Williams-Skipp C, Raman T, Valuck RJ, Watkins H, Palmer BE, Scheinman RI. 2009. Unmasking of a protective tumor necrosis factor receptor I-mediated signal in the collagen-induced arthritis model. Arthritis Rheum 60(2):408–418.

Zhu Y, Gao C, Shen J. 2002. Surface modification of polycaprolactone with poly(methacrylic acid) and gelatin covalent immobilization for promoting its cytocompatibility. Biomaterials 23(24):4889–4895.

Zilla P, Bezuidenhout D, Human P. 2007. Prosthetic vascular grafts: Wrong models, wrong questions and no healing. Biomaterials 28(34): 5009–5027.